

SUPPLEMENTAL FIGURE LEGENDS

Figure S1. Supplemental quantification data and controls.

Quantification of (A) SNB-1::GFP puncta number and (B) size in the command interneuron ventral cord for *odIs1[P_{glr-1}::SNB-1::GFP]* transgenic animals. (C) Quantification of SNB-1::GFP puncta number in the motoneurons for *juIs1[P_{unc-25}::SNB-1::GFP]* transgenic animals. (D) qRT-PCR quantification for relative *glr-1* mRNA levels (normalized to *dIg-1* mRNA controls). N=3 trials. Quantification of the (E) size and (F) number of elongated, internal compartments containing GLR-1::GFP. (G) The mean spontaneous reversal frequency as an indication of GLR-1 function is plotted for the indicated genotypes. (H) The current-voltage relationship (plotted in pA and mV, respectively) for representative recordings from AVA neurons from either a wild-type animal (black line) or an *egl-9(sa307)* mutant (gray line). Red bars indicate normoxia, whereas blue bars indicate hypoxia. ANOVA followed by Dunnett's multiple comparison to wild type, normoxia (*p<0.01). Error bars indicate SEM.

Figure S2. EGL-9E contains a potential C2 domain.

Sequence alignments for *C. elegans* EGL-9E encoded by exons 3 and 4, the C2 domain from the *S. cerevisiae* phospholipase C, and the C2 domain from the mouse PLC δ 3. Conservation of identical and similar amino acids is indicated by black and gray highlighting, respectively.

Figure S3. LIN-10 does not regulate HIF-1 proteins levels or HIF-1 target expression.

Quantification of (A) HIF-1 proteins levels as detected by Western blot from nematode lysates, and (B,C,D) GFP mRNA levels as detected by qRT-PCR from *P_{nhf-57}::GFP* transgenic nematodes for the indicated genotypes. (D) Expression levels were quantified over a time course following initial exposure to hypoxia. ANOVA followed by Dunnett's multiple comparison to wild type, normoxia (*p<0.01).

SUPPLEMENTAL MATERIALS AND METHODS

Strains

The following strains were used: *lin-10(e1439)*, *nuls25[P_{glr-1}::GLR-1::GFP]*, *odIs1[P_{glr-1}::SNB-1::GFP]*, *odIs6[P_{glr-1}::mRFP]*, *odIs22[P_{glr-1}::LIN-10::GFP]*, *juls1[P_{unc-25}::SNB-1::GFP]*, *egl-9(sa307)*, *egl-9(gk277)*, *egl-9(n571)*, *hif-1(ia4)*, *vhl-1(ok161)*, *glr-1(ky176)*, *cdk-5(ok626)*, *cdka-1(gm335)*, *rhy-1(ok1402)*, *ials07[P_{nhr-57}::GFP]*, *ials38[P_{egl-9}::EGL-9::Tag]*, *pzIs2[P_{glr-1}::CDK-5(+)]*, *unc-11(e47)*, *odEx[P_{glr-1}::mRFP::CDK-5]*, *odEx[P_{glr-1}::LIN-10::mCherry]*, *odEx[P_{glr-1}::LIN-10(S/Tmut)::GFP]*, *odEx[P_{glr-1}::rab-5(S23N)]*, *odEx[P_{glr-1}::LIN-10(Pmut)]*, *odEx[P_{glr-1}::LIN-10(Pmut)::GFP]*.

Construction of EGL-9 Isoforms

The individual EGL-9 isoform rescuing constructs EGL-9A, EGL-9E, and EGL-9C were generated by amplifying the 3 SL1s before exons 1, 3 and 5 respectively of genomic *egl-9* from clone WRM0620aA08 and introducing the products into a *glr-1* promoter containing vector. The following forward primers were used to synthesize the constructs: *aaaatgagcagtgcccaaatgatga* (isoform A), *aaaatgatatgcaagtcacttcaacaagtggc* (isoform E), and *aaaatgccattgcgtacaattgtggc* (isoform C). The catalytic site mutant of isoform E was generated by converting His 445 to Ala of the isoform E protein. For localization studies, GFP or mRFP was fused to the amino-terminus in each variant.

Quantitative Real-Time PCR

Total RNAs were extracted with Trizol (Invitrogen Co., Carlsbad, CA). Lysis was done by repeating ten rounds of freezing (by liquid nitrogen) and thawing (at 37 °C). PCR was performed in a iCycler iQ system (Bio-Rad Laboratories Inc., Hercules, CA) using iScript™ One-Step RT-PCR Kit With SYBR® Green (Bio-Rad Laboratories Inc., Hercules, CA) in 20 µL reactions with 20 ng of RNA template. Samples were measured three times and average values were used for the calculation of relative fold changes. The relative levels of *glr-1* mRNA in each preparation were normalized to the levels of *dlg-1* mRNA in each preparation, where the *glr-1/dlg-1* ratio in wild type (*nuls25* alone) was set to 1.

Figure S1. Park, Ghose, et al.

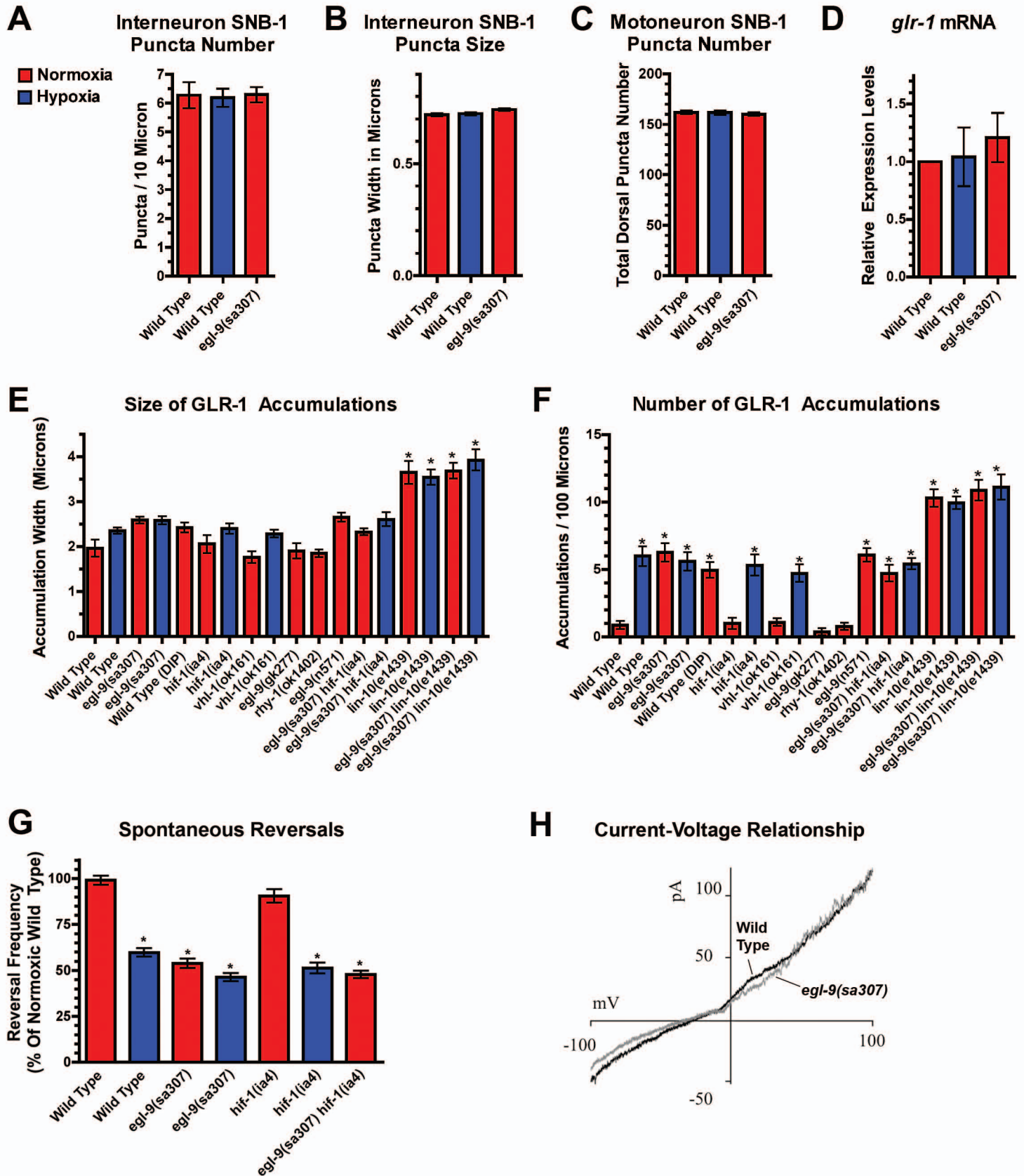


Figure S2. Park, Ghose, et al.

C. elegans EGL-9E exons 3&4
S. cerevisiae Plc1p C2 Domain
Mouse PLC δ 3 C2 Domain

MICKSLQTSGMV--PSNLMPQAAPAVMAP-I-PPTVSFDDPALTTSLLLS
HQPDGSEFKSGYVLKPKKLLPVVTKAKMIPLIYEHFENGSDPVTVKIRILS
GRFLINGQC~~GYVLKP~~-----AYLRQLNTTFD~~PECPGPPRTTLAIQVLT~~

C. elegans EGL-9E exons 3&4
S. cerevisiae Plc1p C2 Domain
Mouse PLC δ 3 C2 Domain

LQNNPILNQT-IS-NFPPTF-SITSKTEPEPSIPIQI--PQRIS----ST
TQLLPRLNDTSPSRNNTNSEV~~KVEE~~FHTDDEPTM~~PISIDK~~GTRISATEAST
AQLPKLN~~AEKPS~~-SIVDPI~~VRVEIH~~-----GVPEDCAQKET

C. elegans EGL-9E exons 3&4
S. cerevisiae Plc1p C2 Domain
Mouse PLC δ 3 C2 Domain

--S----TVP-FSSEGS-AFKPYRNT-HVFNSISSE-S-----MSSMCTS
KSSQGN~~GFNPIWDAEVSITLKD~~DTDLTFIKFMVISEETQ-----IASVCLK
DYVLNNGFNPCWEQTLQFRLRAPELVLVRFVVEDYDTTSPNDFVQGSTLP

C. elegans EGL-9E exons 3&4
S. cerevisiae Plc1p C2 Domain
Mouse PLC δ 3 C2 Domain

HEASLEHMSSASL-AM---FPTSSTAQSDISRL
LN~~YL~~RMGYRHIPLFNMEGEQYIFCTLFIHTQIL
LSSLKQGYRHIHLLSKDGASLAPATL~~FVHIRIQ~~

Figure S3. Park, Ghose, et al.

